A&A 453, 943–947 (2006)
DOI: 10.1051/0004-6361:20054736

Astronomy & Astrophysics

Electron temperature fluctuations in H II regions

The feasibility of t^2 estimates from point-to-point observations⋆

M. V. F. Copetti

Laboratório de Análise Numérica e Astrofísica, Departamento de Matemática, Universidade Federal de Santa Maria, 97119-900 Santa Maria, RS, Brazil
e-mail: mvfc@lana.ccne.ufsm.br

Received 20 December 2005 / Accepted 24 February 2006

ABSTRACT

Context. The spatial electron temperature fluctuations in ionized nebulae that were initially proposed to explain the discrepancies among temperatures obtained from different sensors have been pointed to as the cause of huge inconsistencies among abundances of heavy elements calculated from recombination and forbidden emission lines. Recently, there have been some attempts of direct detection and quantification of spatial temperature fluctuations with point-to-point temperature measurements across the nebula.
Aims. In this paper, we assess the feasibility of estimating the temperature fluctuation parameter t^2, the total variance of the spatial distribution of temperature relative to the mean, from the distribution of temperatures measured on the plane of the sky with different sensors.
Methods. Point-to-point measurements of the electron temperature at a series of contiguous and equally spaced rectangular apertures along a radius of homogeneous and spherically symmetric nebulae were numerically simulated for six different temperature sensors.
Results. Variances of projected temperature distributions were obtained and compared with total t^2 for different values for the density, ionization parameter and temperature of the ionizing star. The projected profiles of electron temperature obtained from indicators associated with ions occurring at large fractions of the nebula, such as [O III] $(\lambda4959+\lambda5007)/\lambda4363$, [Ar III] $(\lambda7136+\lambda7751)/\lambda5192$, and the Balmer jump $(I_\lambda(3646^-) - I_\lambda(3646^+))/\mathrm{H}\beta$, are good tracers of the internal gradient of temperature. The variances t_s^2 of the projected temperature distributions measured from these sensors correspond to significant fractions of the total temperature variance, for typical nebulae of the order of $t_s^2/t^2 \approx 30\%$, 25%, and 15% for the Balmer jump and the [O III] and [Ar III] ratios, in that order. On the other hand, the temperature profiles obtained from sensors corresponding to low ionization ions, such as [N II] $(\lambda6548 + \lambda6584)/\lambda5755$, [O I] $(\lambda6300 + \lambda6364)/\lambda5577$, and [C I] $(\lambda9823 + \lambda9849)/\lambda8728$, are almost constant at the values of temperature of the outer parts of the nebula, fail to reproduce the true temperature gradient, and have a t_s^2 that is always less than 10% and is usually around 1–3% of t^2.

Key words. ISM: H II regions – ISM: planetary nebulae: general

1. Introduction

The theory of photoionized nebulae very successfully explains most of the features observed in the spectra of H II regions and planetary nebulae. This fact has supported the intensive use of these objects as probes of the chemical composition of galaxies. Traditionally, the abundances of heavy elements in ionized nebulae have been obtained from their strong, collisionally excited emission lines. The recent developments in astronomical instruments have made the determination of the abundances of the C, N, and O elements from their weak recombination lines possible. However, huge discrepancies between the abundances obtained from collisionally excited and recombination lines have been found, which cast doubt on the accuracy of the abundance determinations in gaseous nebulae. For example, Liu et al. (1995) determined abundances of C, N, and O in the planetary nebula NGC 7009 by recombination lines and found that they are about 5 times higher than those derived from forbidden lines.

The existence of spatial temperature fluctuations in the nebulae has been suggested as one of the most probable explanations of the inconsistency among abundances calculated from forbidden and recombination lines (Peimbert et al. 1995). Originally, large temperature fluctuations had been proposed by Peimbert (1967) to explain the discrepancies between the values of electron temperature obtained from different indicators.

The magnitude of the temperature fluctuations are usually quantified by the parameter t^2 defined by Peimbert (1967) as

$$t^2 = \frac{\int (T_\mathrm{e} - T_0)^2 N_\mathrm{i} N_\mathrm{e} \mathrm{d}V}{T_0^2 \int N_\mathrm{i} N_\mathrm{e} \mathrm{d}V}, \quad (1)$$

with

$$T_0 = \frac{\int T_\mathrm{e} N_\mathrm{i} N_\mathrm{e} \mathrm{d}V}{\int N_\mathrm{i} N_\mathrm{e} \mathrm{d}V}, \quad (2)$$

where N_i is the density of the ion used to measure the temperature, and where the integrals are calculated over the volume V of the nebula. Essentially, T_0 and t^2 are the mean and the relative variance of the temperature distribution weighted by the square of the local density.

However, the magnitudes of the temperature fluctuations needed to reconcile the recombination line metallicities with

⋆ Figures 6–15 are only available in electronic form at http://www.edpsciences.org

Table 1. Electron temperature indicators and symbols.

Spectroscopic index	Temperature symbols
$(I_\lambda(3646^-) - I_\lambda(3646^+))/\mathrm{H}\beta$	T_e(Bac)
[O III] (λ4959 + λ5007)/λ4363	T_e(O III)
[N II] (λ6548 + λ6584)/λ5755	T_e(N II)
[O I] (λ6300 + λ6364)/λ5577	T_e(O I)
[Ar III] (λ7136 + λ7751)/λ5192	T_e(Ar III)
[C I] (λ9823 + λ9849)/λ8728	T_e(C I)

those based on collisionally excited lines or the electron temperature measurements from different line ratios of planetary nebulae and H II regions of the order $t^2 \approx 0.02$–0.10 (Dinerstein et al. 1985; Liu & Danziger 1993; Peimbert et al. 1995; Esteban et al. 1998, 1999a,b; Luridiana et al. 1999; Gonzalez-Delgado et al. 1994) are considerably higher than those predicted by standard photoionisation models (Gruenwald & Viegas 1995; Kingdon & Ferland 1995; Pérez 1997), which are typically in the range of $t^2 \leq 0.02$. Besides, the physical mechanisms that could possibly explain the large temperature fluctuations presumed are unknown. Recently, an alternative solution to the abundance problem has been proposed and supported based on the assumption of the presence of hydrogen-deficient and very cold clumps inside the nebula, which, even if they were to make up only a few percent of the total mass, would be largely responsible for the emission of recombination lines of heavy elements (Liu et al. 2000; Tsamis & Péquignot 2005; Tsamis et al. 2004). So, the question of the existence of substantial spatial variations of electron temperature in nebulae has became a key issue in the study of H II regions and planetary nebulae.

There have been some attempts of estimating the magnitude of the temperature fluctuations from point-to-point measurements of the temperature in planetary nebulae and H II regions (Liu 1998; Krabbe & Copetti 2002; O'Dell et al. 2003; Rubin et al. 2002, 2003). As a direct estimator for t^2, Liu (1998) has proposed the use of

$$t_\mathrm{s}^2 = \frac{\sum_{i=1}^{N} (T_\mathrm{e}^i - T_0)^2 F_\mathrm{i}(\mathrm{H}\beta)}{T_0^2 \sum_{i=1}^{N} F_\mathrm{i}(\mathrm{H}\beta)}, \quad (3)$$

where T_e^i and $F_\mathrm{i}(\mathrm{H}\beta)$ are the electron temperature and the Hβ flux obtained for the aperture i, respectively, and where N is the total number of apertures. Clearly, this parameter is a biased estimator of t^2. We have that $t_\mathrm{s}^2 \leq t^2$, since the temperature measured at any aperture is a mean value inside a cylinder through the nebula. So, any line of sight or small-scale temperature fluctuation would be smoothed out by this kind of observation. For this reason, it is clear that t_s^2 can only give a lower limit to t^2. In the present paper, by means of model simulations, we assess the feasibility and discuss the limitations of the t^2 estimations based on point-to-point measurements of the electron temperature in ionized nebulae.

2. The models

We have numerically simulated a point-to-point measurement of the electron temperature at a series of contiguous and equally spaced rectangular apertures along the radius of a homogeneous and spherically symmetric nebula. Six different electron temperature sensors were considered, including the most commonly used [O III](λ4959 + λ5007)/λ4363, [N II](λ6548 + λ6584)/λ5755, and the Balmer jump at 3646 Å relative to Hβ (see Table 1 for the complete list and for the symbols used for the derived temperatures). The photoionization code Cloudy 95.03 (Ferland et al. 1998) was used to calculate the thermal and ionization structure of the nebula. An inner radius of 10% of the outer nebular radius was assumed. The non-LTE CoStar stellar atmosphere models (Schaerer et al. 1996a,b; Schaerer & Koter 1997) for zero age main sequence stars were used. The solar chemical composition was adopted. We ran models with the effective temperature of the ionizing star varying from 38 500 to 50 000 K, corresponding to spectral type from O8 to O3, according to the calibration of Vacca et al. (1996), an with an ionization parameter in the range $-3.5 \leq \log U \leq -2$ and a hydrogen density $1.5 \leq \log N_\mathrm{H}\,(\mathrm{cm}^{-3}) \leq 4$. Also, to test the effects of spatial resolution on the simulations, we varied the number of apertures in the range $5 \leq N \leq 1000$.

The emissivities of the emission lines involved were calculated with an n-level atom programme ($5 \leq n \leq 10$) that we wrote using the atomic parameters from the *IRAF/STSDAS 3.0/nebular* package database. For the fainter lines (e.g. [O III]λ4363 or [N II]λ5755), we considered the contributions to the emissivities due to recombination and charge transfer effects, since they are significant at some parts of the nebula. The emissivity of the Balmer jump was calculated from T_e (in K units) and the Hβ emissivity predicted by the code Cloudy by the expression

$$\frac{j_\nu(\mathrm{Bac})}{j_{\mathrm{H}\beta}} = 2.00 \times 10^{-12}\, 10^{424/T_\mathrm{e}} T_\mathrm{e}^{-0.517} \quad (\mathrm{in\ Hz}^{-1}), \quad (4)$$

deduced from the approximations given by Aller (1984, p. 76 and 99). The emissivities were integrated within the apertures and along the line of sight to produce the emission line intensities. The simulated line ratios and the Balmer discontinuity were used to derive the "observed" electron temperature in each aperture using the same n-level atom models and numerically solving Eq. (4) for T_e(Bac).

3. Results and discussions

In Fig. 1, the comparison between the true electron temperature radial gradient and the spatial profiles of temperature obtained from different sensors is shown for a typical example of the simulations described in Sect. 2. This figure shows that the temperature indicators can be divided into two groups. The electron temperature profiles derived from indicators associated with ions occurring at large fractions of the nebula, such as T_e(Bac), T_e(O III), and T_e(Ar III), tend to follow the true internal temperature variation fairly well. On the other hand, the spatial profiles of temperatures obtained from line ratios of low ionization ions, T_e(N II), T_e(O I), and T_e(C I), are almost constant, at values representative of the higher temperatures predicted for the outskirts of the nebula, and badly fail to reproduce the inner part of the electron temperature gradient, essentially because the low ionization ions are concentrated in the outer and hotter parts of the nebula.

Using expression (3), we calculated the relative variance t_s^2 of the temperature profile for each temperature sensor considered, then compared them with the value of t^2. The level of dependency of t_s^2 on the number of apertures N is summarised in Table 2, which shows the range of the percentage values of t_s^2 for $N = 5$, 10, and 20, relative to t_s^2 for $N = 100$, found in the simulations. We verified that t_s^2 calculated from T_e(Bac), T_e(O III), and T_e(Ar III) are little dependent on the number of apertures, especially for $N \geq 10$. Even for as a small number

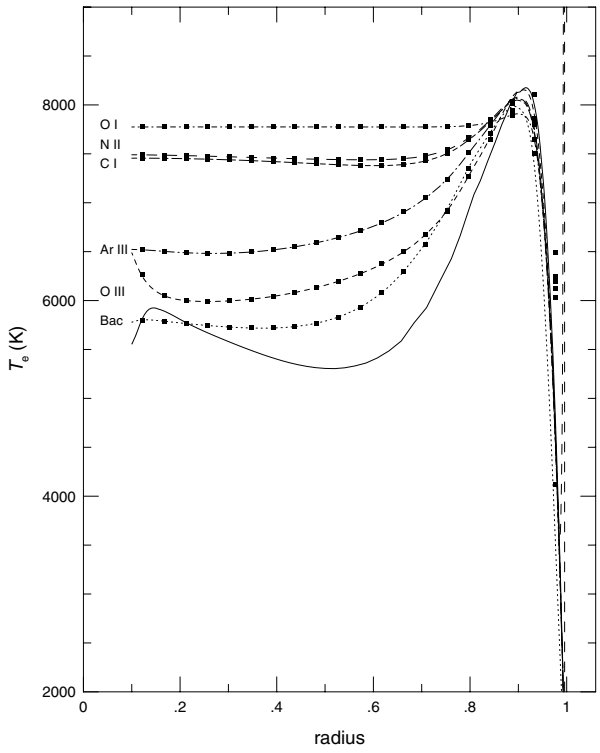

Fig. 1. Comparison between the true electron temperature radial gradient (solid line) and the "observed" spatial profiles of temperature obtained from different sensors with a very large number of apertures, $N = 1000$ (broken lines), and with a small one, $N = 20$ (marks). The input parameters for this model were: $T_{\rm eff} = 43\,560$ K, $\log U = -3$, and $N_{\rm e} = 100$ cm^{-3}. The spike in the $T_{\rm e}$(N II) profile at the outskirts of the nebula, which is the consequence of a strong enhancement of the [N II]λ5755 emission line by charge transfer effects in a more than 95% neutral thin layer, is impractical to observe, because the corresponding [N II] lines are extremely weak, and has a negligible effect on the value calculated for $t^2_{\rm s}$(N II), due to the flux weighting.

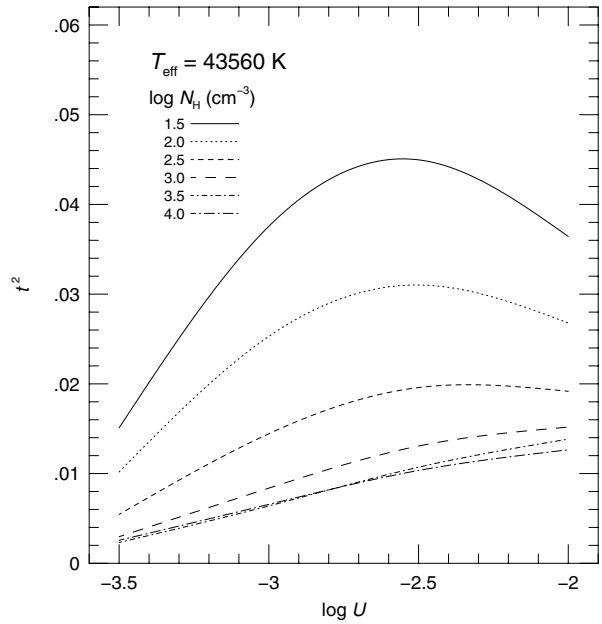

Fig. 2. Temperature fluctuation parameter t^2 vs. the ionization parameter U for $T_{\rm eff} = 43\,560$ K and six different values of hydrogen density in the range $1.5 \le \log N_{\rm H}\,({\rm cm}^{-3}) \le 4$.

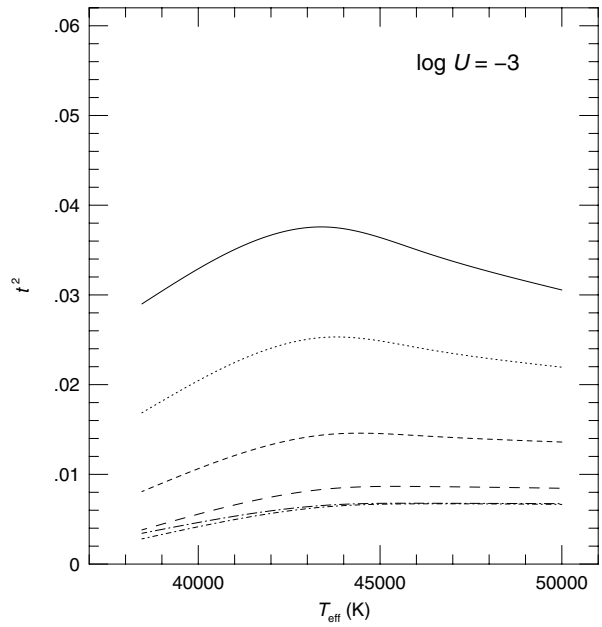

Fig. 3. Temperature fluctuation parameter t^2 vs. the effective temperature $T_{\rm eff}$ of the ionizing star for an ionization parameter $\log U = -3$ and six different values of hydrogen density in the range $1.5 \le \log N_{\rm H}\,({\rm cm}^{-3}) \le 4$ (indicated by the same line types used in Fig. 2).

as $N = 5$, these sensors produce reasonable results, with $t^2_{\rm s}$ at least 60% of the value for $N = 100$. This is a consequence of the fact that the photoionization models predict a fairly smooth gradient of temperature with steep spatial variations only at the outer border of the nebula (see Fig. 1).

Figures 2 and 3 show the dependence of the electron temperature fluctuation parameter t^2 on the ionization parameter U for a fixed stellar temperature, $T_{\rm eff} = 43\,560$ K, and on the effective temperature of the ionizing star for a fixed ionization parameter, $\log U = -3$, and for 6 different values of hydrogen density in the range $1.5 \le \log N_{\rm H}\,({\rm cm}^{-3}) \le 4$, respectively. These figures illustrate the kind of relationships between t^2, U, $T_{\rm eff}$, and $N_{\rm H}$ found in the complete set of models. The t^2 parameter ranges from 0.001 to 0.05, with little dependency on the stellar effective temperature, but strong dependency on the hydrogen density for $\log N_{\rm H}\,({\rm cm}^{-3}) \lesssim 3$. According to the models, denser objects would have more homogeneous temperature structures, and consequently lower values of t^2. The increase of temperature in the outer parts of the nebula (see Fig. 1), caused by the hardening of the ionizing radiation as the distance to the centre increases, which is due to the preferential absorption of low-energy photons in the photoionization process, is more pronounced in rarefied objects, for which the ionizations are essentially produced by photons coming directly from the stars. For denser objects, the much softer diffuse radiation field plays a more important role in the ionization of the nebula.

In Figs. 4 to 15, we summarise the results of our simulated evaluation of the spatial variance of the electron temperature obtained from point-to-point measurements of temperature. In these figures, the $t^2_{\rm s}$ parameter for each of the six electron temperature sensors listed in Table 1 is shown as a function of the ionization parameter U (for $T_{\rm eff} = 43\,560$ K) or stellar temperature (for $\log U = -3$) for a number of apertures $N = 100$ and different values of electron density. For all temperature sensors considered, the ratio $t^2_{\rm s}/t^2$ showed little dependence on the stellar temperature, especially for $T_{\rm eff} \gtrsim 43\,000$ K. Again, the electron temperature sensors can be divided into two groups.

Table 2. Dependency of t_s^2 on the number of apertures N.

	$t_s^2(N)/t_s^2(N' = 100)$ (per cent)					
N	Bac	O III	N II	O I	Ar III	C I
5	60–90	62–91	45–88	00–27	70–98	28–83
10	85–97	84–96	67–92	25–56	83–99	58–87
20	97–99	94–99	84–94	41–78	92–99	79–92

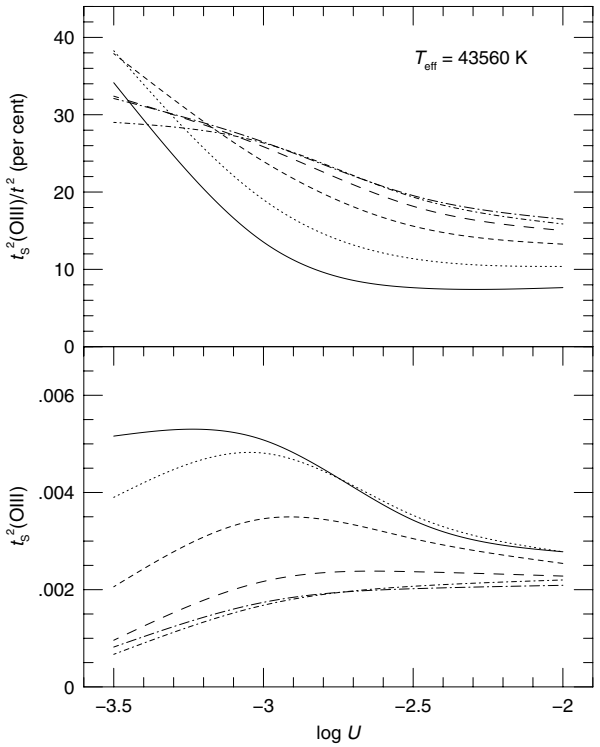

Fig. 4. Temperature fluctuation parameter of the simulated measurements of T_e(O III) (in percentages of t^2 in the upper panel and absolute value in the lower panel) vs. the ionization parameter U for $N = 100$ apertures, $T_{eff} = 43\,560$ K, and six different values of hydrogen density in the range $1.5 \leq \log N_H\,(cm^{-3}) \leq 4$ (indicated by the same line types used in Fig. 2).

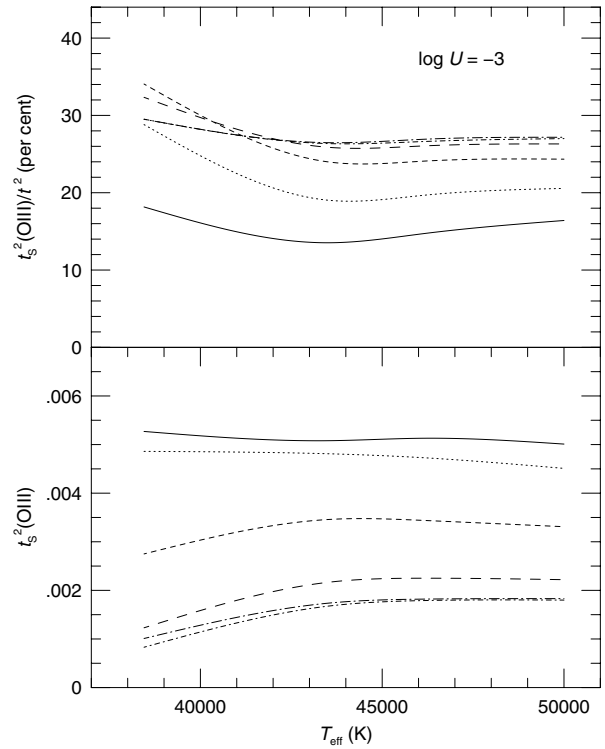

Fig. 5. Temperature fluctuation parameter of the simulated measurements of T_e(O III) (in percentages of t^2 in the upper panel and absolute value in the lower panel) vs. the effective temperature T_{eff} of the ionizing star for $N = 100$ apertures, ionization parameter $U = -3$, and six different values of hydrogen density in the range $1.5 \leq \log N_H\,(cm^{-3}) \leq 4$ (indicated by the same line types used in Fig. 2).

The temperature variances t_s^2 from T_e(Bac), T_e(O III), and T_e(Ar III) correspond to a significant fraction of t^2 of the order of 20−40%, 8−40%, and 5−22%, in that order. On the other hand, for the sensors associated with low ionization ions, T_e(N II), T_e(O I), and T_e(C I), t_s^2 is always less than 10% and is usually around 1−3% of t^2.

To show the potential use of the present simulations, we have estimated the global t^2 from the measured values of t_s^2(O III) for 30 Doradus and the Orion Nebulae. From the calibration of the ionization parameter with the line ratio [S II](λ6717 + λ6731)/[S III](λ9069 + λ9532) by Diaz et al. (1991), and the observed line ratios from Kennicutt et al. (2000), we estimate a value of $\log U \approx -3.2$ for both of these objects. The electron density is $\log N_e\,(cm^{-3}) = 3.7 \pm 0.2$ (Esteban et al. 1998) in the Orion Nebula and $\log N_e\,(cm^{-3}) = 2.5 \pm 0.1$ (Peimbert 2003) in 30 Doradus. The spectral type of the main ionizing stars is O6 or O7 V in the Orion Nebula (Conti & Alschuler 1971; Copetti & Bica 1983) and O3 in 30 Doradus (Massey & Hunter 1998), which correspond to $T_{eff} \approx 40\,000$ K and 50 000 K, respectively, according to the calibration of Vacca et al. (1996). From Fig. 5, we verify that t_s^2(O III) is 24% of t^2 for the 30 Doradus Nebula and 28% of t^2 for the Orion Nebula.

From point-to-point measurements in three different directions on the plane of 30 Doradus Nebula, Krabbe & Copetti (2002) found a fairly homogeneous spatial distribution of [O III] electron temperature, corresponding to t_s^2(O III) = 0.0025. Therefore, we estimate a value of $t^2 = 0.010$ for this nebula, which is very close to the value of $t^2 = 0.014$ predicted by the photoionization model with appropriate parameters. Similar observations by Tsamis et al. (2003) confirmed that the spatial variation of temperature is very small in this nebula. However, based on the comparisons among electron temperatures obtained from forbidden lines and from the Balmer continuum, as well as among O^+, O^{++}, and C^+ ionic abundances obtained from forbidden and recombination lines, Peimbert (2003) estimated $t^2 = 0.033 \pm 0.005$ for 30 Doradus.

For the Orion Nebula, from the value of t_s^2(O III) = 0.0079 measured by O'Dell et al. (2003), we derive $t^2 = 0.028$, which is the same value as that obtained by O'Dell et al. (2003) using a completely different approach. They evaluated the temperature fluctuation for the whole nebula from the projected [O III] temperature distribution, based essentially on the fraction of the nebular volume occupied by the O^{++} zone and on the difference between the mean temperatures in the O^+ and O^{++} zones. Through long-slit spectroscopy, Rubin et al. (2003) have obtained eight independent estimates of t_s^2(O III) for four different $52'' \times 0.5''$ areas over the Orion Nebula, finding values from 0.00682 to 0.0176, which correspond to t^2 varying from 0.024 to 0.062, according to our models. The two highest values for t_s^2(O III) were found for the fainter areas, consequently from data with poorer S/N. The median of their estimates from brighter areas, t_s^2(O III) = 0.0098, is probably more representative of the whole nebula, and it leads to $t^2 = 0.035$.

Esteban et al. (1998) estimated $t^2 = 0.024 \pm 0.004$ from the comparison of O^{++} abundances from collisionally excited and recombination lines.

Although a more profound discussion about the existence of significant temperature fluctuations in ionized nebulae is beyond the scope of this paper, we observe that two different conclusions were attained from the above comparisons. For the 30 Doradus Nebula, we estimate a value of t^2, compatible with that predicted by photoionization models, but too small to invoke the temperature fluctuations as the cause of the discrepancy between the abundances derived from collisionally excited and recombination lines. On the other hand, for the Orion Nebula, we obtain a magnitude for the temperature fluctuation that could explain the abundance problem, but it is much higher than the predictions of photoionization models for homogeneous nebulae. If the projected temperature variance observed in the Orion Nebula is confirmed (the knotty task is the discount of the pure error variance), it would leave no doubt that the classic temperature fluctuations play an important role in the interpretation of the spectra of H II regions. 2D mapping of temperature with different indicators for a significant sample of objects would be of help to settle the question.

4. Conclusions

Through model simulations, we have assessed the feasibility of quantifying the global spatial temperature fluctuation parameter t^2, based on point-to-point measurements of the electron temperature across the nebula with different temperature sensors. The main conclusions are:

1. The projected profiles of electron temperature obtained from sensors associated with ions occurring in large fractions of the nebula, such as T_e(Bac), T_e(O III), and T_e(Ar III), are good tracers of the internal gradient of temperature. On the other hand, the temperature profiles obtained from temperature sensors corresponding to low ionization ions, such as T_e(N II), T_e(O I), and T_e(C I), are almost constant, at values corresponding to the temperatures of the outer parts of the nebula, and fail to reproduce the true temperature gradient.
2. The variances t_s^2 of the distributions of the temperatures T_e(Bac), T_e(O III), and T_e(Ar III), measured on the plane of the sky, correspond to a significant fraction of the total temperature fluctuation t^2. For typical H II regions ($40\,000 \lesssim T_{\rm eff} \lesssim 50\,000$ K, $N_e \approx 100$–1000 cm^{-3}, and $\log U \approx -3$), $t_s^2/t^2 \approx 30\%$, 25%, and 15% for the distributions of T_e(Bac), T_e(O III), and T_e(Ar III), in that order. On the other hand, for the sensors associated with low ionization ions, T_e(N II), T_e(O I), and T_e(C I), $t_s^2/t^2 \approx 2\%$.

Acknowledgements. This work was partially supported by the Brazilian institutions CNPq and FAPERGS. We thank the anonymous referee for helpful comments and suggestions.

References

Aller, L. H. 1984, Physics of Thermal Gaseous Nebulae (Dordrecht: Reidel)
Conti, P. S., & Alschuler, W. R. 1971, ApJ, 170, 325
Copetti, M. V. F., & Bica, E. L. D. 1983, Ap&SS, 91, 381
Diaz, A. I., Terlevich, E., Vilchez, J. M., Pagel, B. E. J., & Edmunds, M. G. 1991, MNRAS, 253, 245
Dinerstein, H. L., Lester, D. F., & Werner, M. W. 1985, ApJ, 291, 561
Esteban, C., Peimbert, M., Torres-Peimbert, S., & Escalante, V. 1998, MNRAS, 295, 401
Esteban, C., Peimbert, M., Torres-Peimbert, S., García-Rojas, J., & Rodríguez, M. 1999a, ApJS, 120, 113
Esteban, C., Peimbert, M., Torres-Peimbert, S., & Rodríguez, M. 1999b, Rev. Mex. Astron. Astrofis., 35, 65
Ferland, G. J. 2001, PASP, 113, 41
Ferland, G. J., Korista, K. T., Verner, D. A., et al. 1998, PASP, 110, 761
Gonzalez-Delgado, R. M., Perez, E., Tenorio-Tagle, G., et al. 1994, ApJ, 437, 239
Gruenwald, R., & Viegas, S. M. 1995, A&A, 303, 535
Kennicutt, R. C., Bresolin, F., French, H., & Martin, P. 2000, ApJ, 537, 589
Kingdon, J. B., & Ferland, G. J. 1995, ApJ, 450, 691
Krabbe, A. C., & Copetti, M. V. F. 2002, A&A, 387, 295
Liu, X.-W. 1998, MNRAS, 295, 699
Liu, X., & Danziger, J. 1993, MNRAS, 263, 256
Liu, X.-W., Storey, P. J., Barlow, M. J., & Clegg, R. E. S. 1995, MNRAS, 272, 369
Liu, X.-W., Storey, P. J., Barlow, M. J., et al. 2000, MNRAS, 312, 585
Luridiana, V., Peimbert, M., & Leitherer, C. 1999, ApJ, 527, 110
Massey, P., & Hunter, D. A. 1998, ApJ, 493, 180
O'Dell, C. R., Peimbert, M., & Peimbert, A. 2003, AJ, 125, 2590
Peimbert, A. 2003, ApJ, 584, 735
Peimbert, M. 1967, ApJ, 150, 825
Peimbert, M., Torres-Peimbert, S., & Luridiana, V. 1995, Rev. Mex. Astron. Astrofis., 31, 131
Pérez, E. 1997, MNRAS, 290, 465
Rubin, R. H., Bhatt, N. J., Dufour, R. J., et al. 2002, MNRAS, 334, 777
Rubin, R. H., Martin, P. G., Dufour, R. J., et al. 2003, MNRAS, 340, 362
Schaerer, D., & de Koter, A. 1997, A&A, 322, 598
Schaerer, D., de Koter, A., Schmutz, W., & Maeder, A. 1996a, A&A, 310, 837
Schaerer, D., de Koter, A., Schmutz, W., & Maeder, A. 1996b, A&A, 312, 475
Tsamis, Y. G., & Péquignot, D. 2005, MNRAS, 364, 687
Tsamis, Y. G., Barlow, M. J., Liu, X.-W., Danziger, I. J., & Storey, P. J. 2003, MNRAS, 338, 687
Tsamis, Y. G., Barlow, M. J., Liu, X.-W., Storey, P. J., & Danziger, I. J. 2004, MNRAS, 353, 953
Vacca, W. D., Garmany, C. D., & Shull, J. M. 1996, ApJ, 460, 914

Online Material

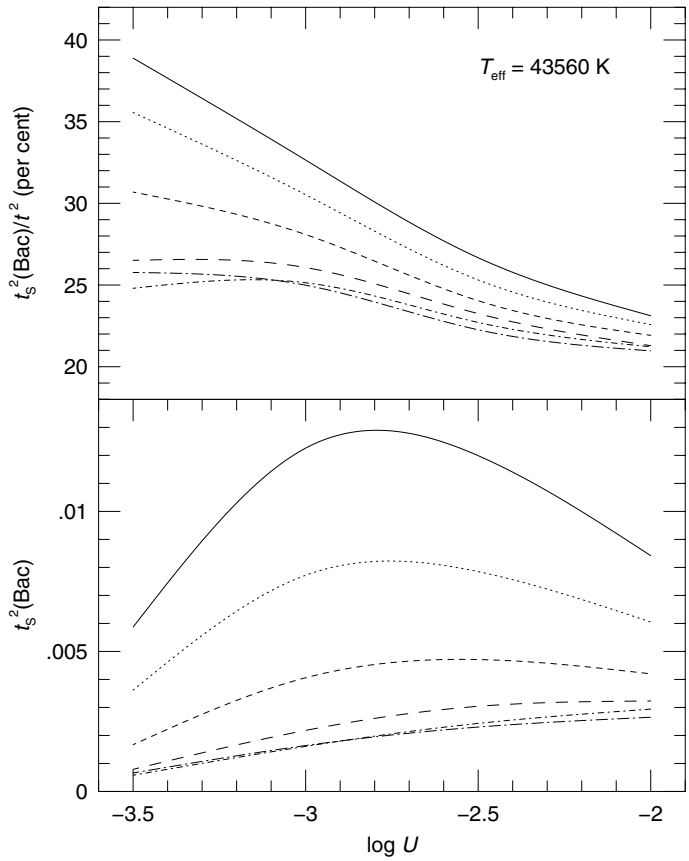

Fig. 6. The same as in Fig. 4, except for temperature T_e(Bac).

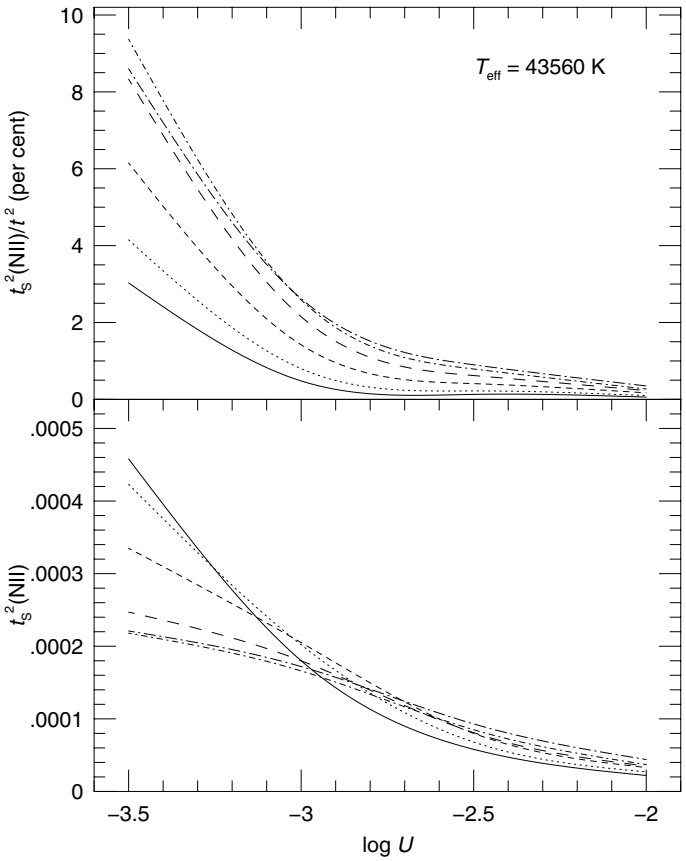

Fig. 8. The same as in Fig. 4, except for temperature T_e(N II).

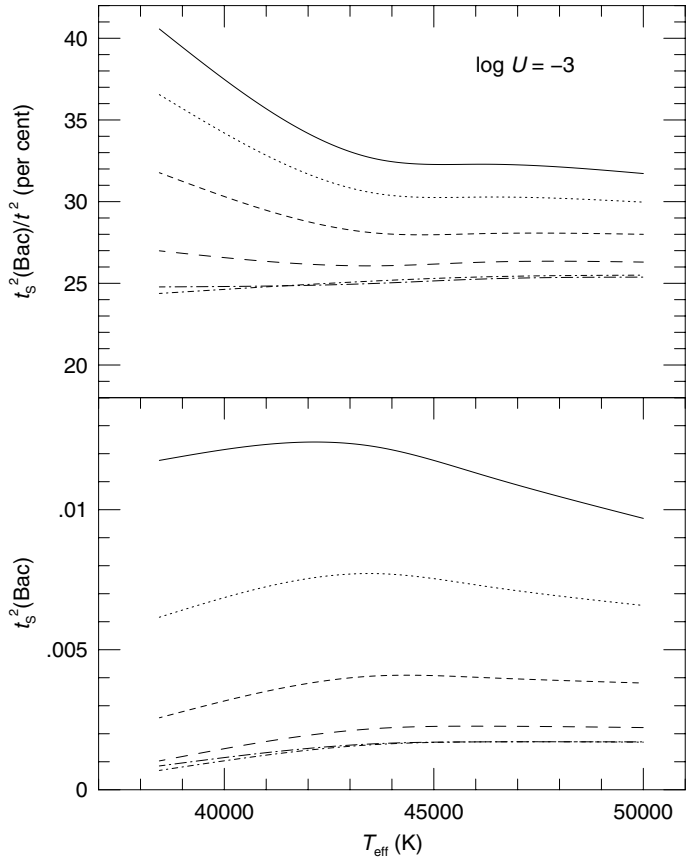

Fig. 7. The same as in Fig. 5, except for temperature T_e(Bac).

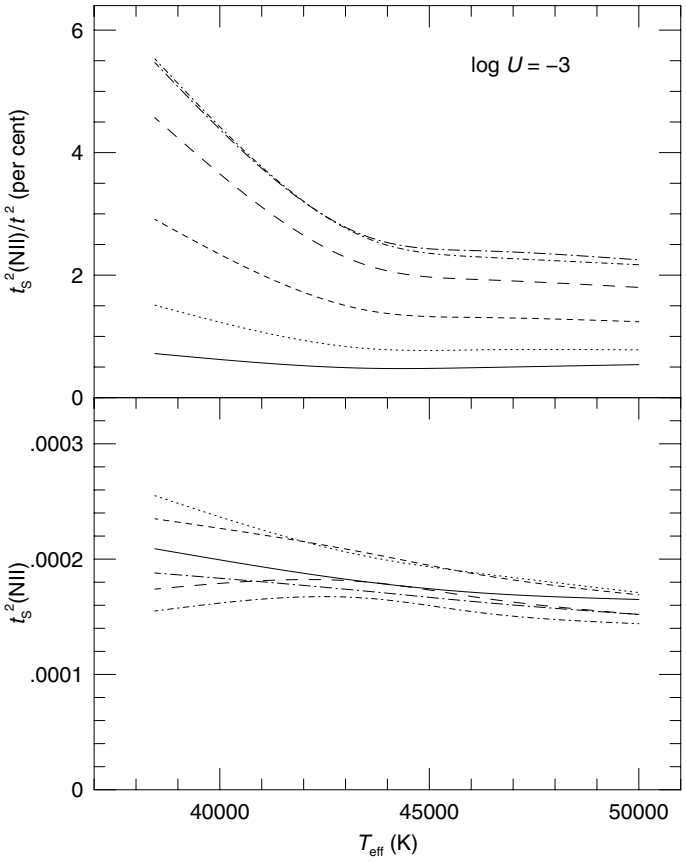

Fig. 9. The same as in Fig. 5, except for temperature T_e(N II).

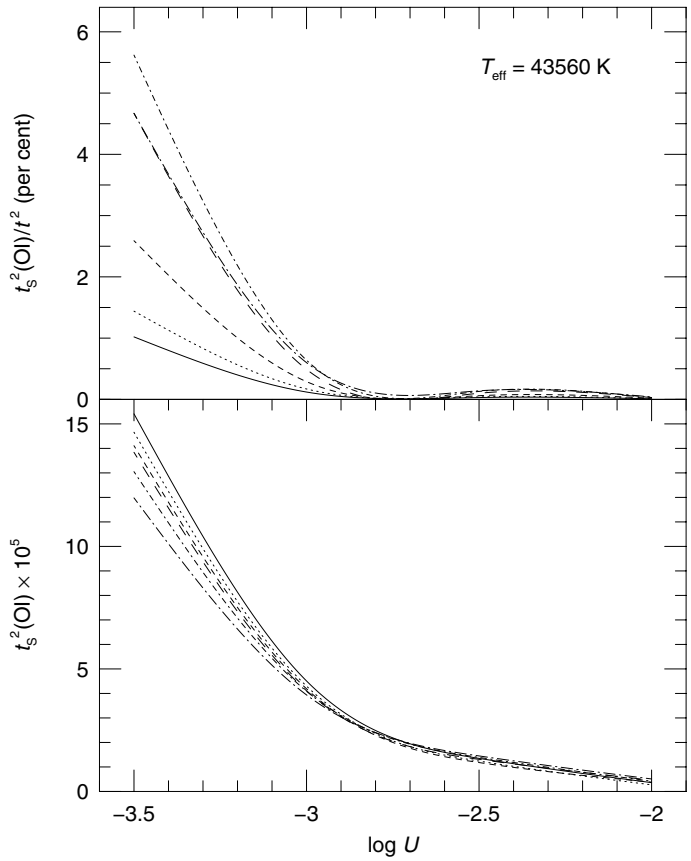

Fig. 10. The same as in Fig. 4, except for temperature T_e(O I).

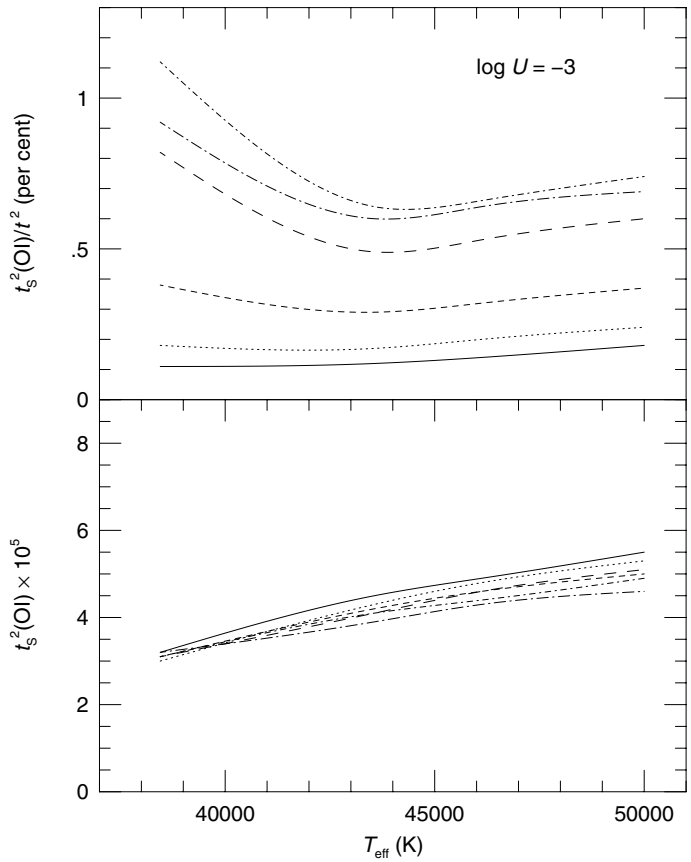

Fig. 11. The same as in Fig. 5, except for temperature T_e(O I).

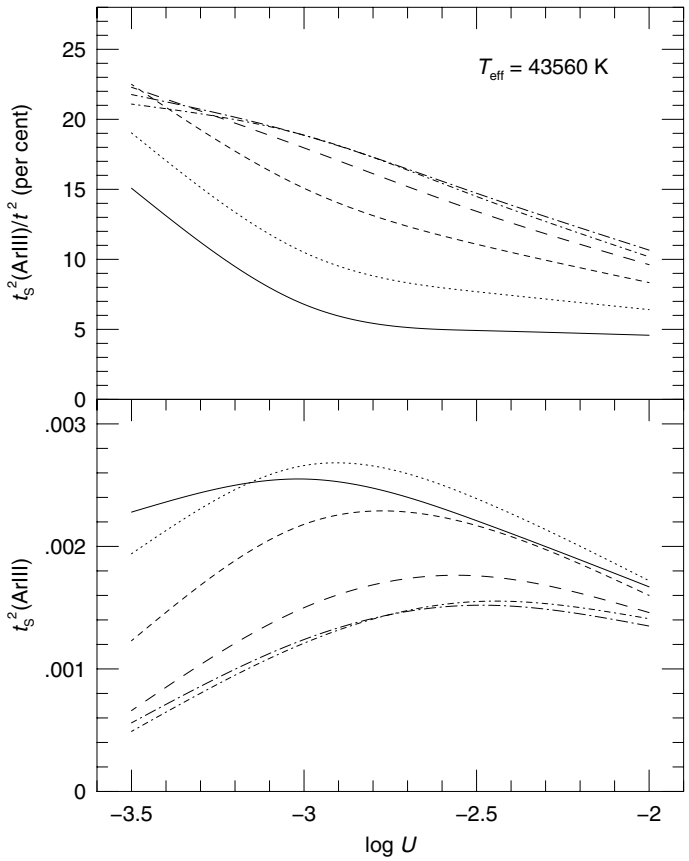

Fig. 12. The same as in Fig. 4, except for temperature T_e(Ar III).

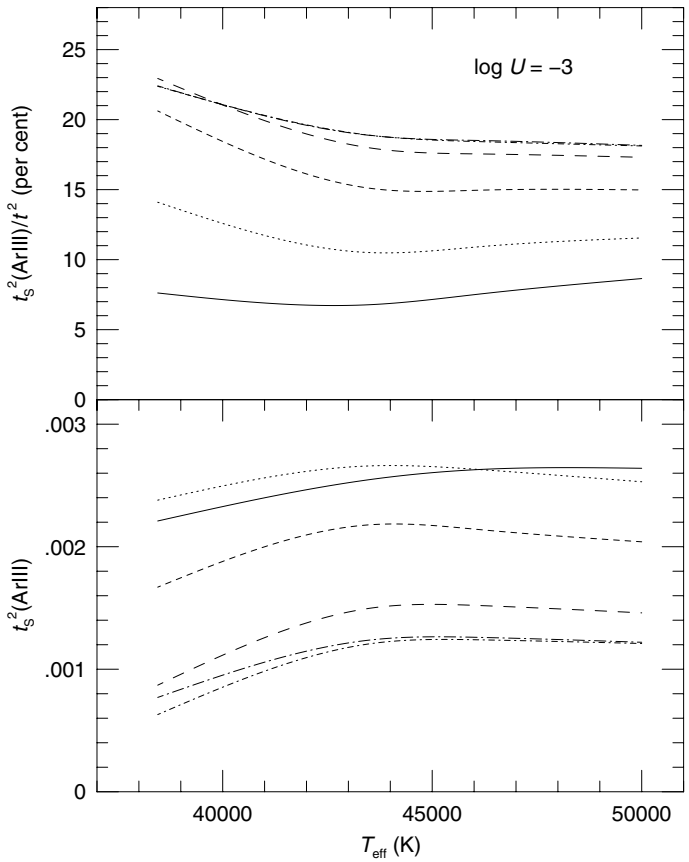

Fig. 13. The same as in Fig. 5, except for temperature T_e(Ar III).

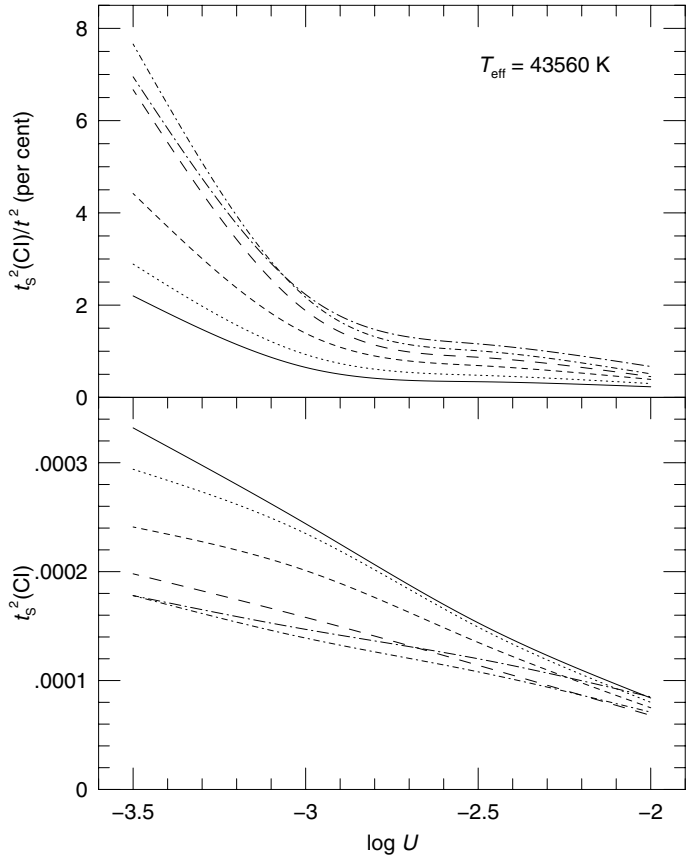

Fig. 14. The same as in Fig. 4, except for temperature T_e(C I).

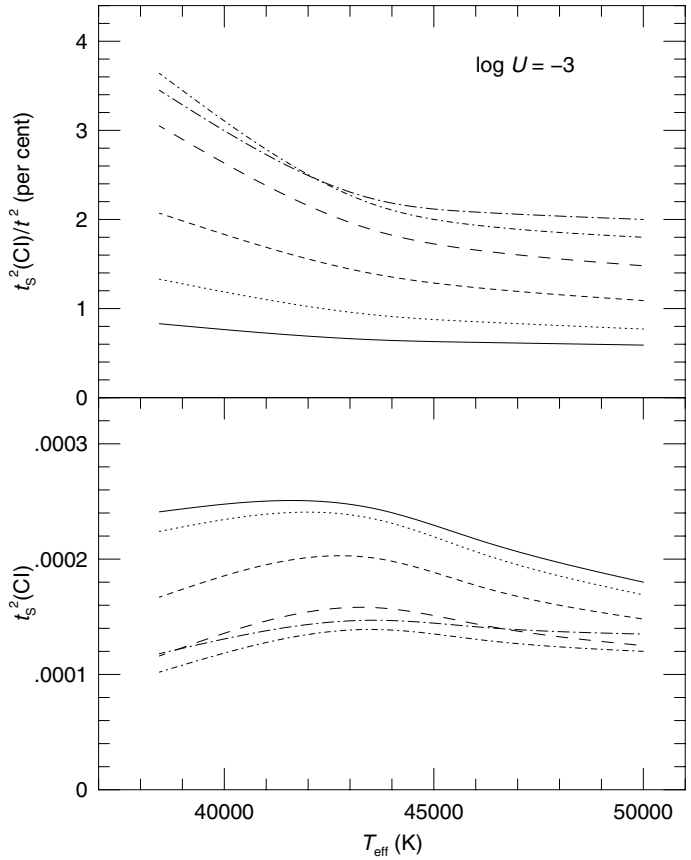

Fig. 15. The same as in Fig. 5, except for temperature T_e(C I).